Supplemental Material

Journal of Climate
The Role of Anthropogenic Aerosol Forcing in the 1850–1985 Strengthening of the AMOC in CMIP6 Historical Simulations
https://doi.org/10.1175/JCLI-D-22-0124.1

© Copyright 2022 American Meteorological Society (AMS)
For permission to reuse any portion of this work, please contact permissions@ametsoc.org. Any use of material in this work that is determined to be "fair use" under Section 107 of the U.S. Copyright Act (17 USC §107) or that satisfies the conditions specified in Section 108 of the U.S. Copyright Act (17 USC §108) does not require AMS's permission. Republication, systematic reproduction, posting in electronic form, such as on a website or in a searchable database, or other uses of this material, except as exempted by the above statement, requires written permission or a license from AMS. All AMS journals and monograph publications are registered with the Copyright Clearance Center (https://www.copyright.com). Additional details are provided in the AMS Copyright Policy statement, available on the AMS website (https://www.ametsoc.org/PUBSCopyrightPolicy).

Supplementary information for 'The role of anthropogenic aerosol forcing in driving a strengthening of the externally-forced AMOC up to 1985 in CMIP6 historical simulations'

Jon Robson, Matthew B. Menary, Rowan T. Sutton, Jenny Mecking,

Jonathan M. Gregory, Colin Jones, Bablu Sinha, David P. Stevens, and Laura W. Wilcox

June 1, 2022

1 Models used

Table S1: The CMIP6 models used in this study, the number of ensemble members used, and their ASR_HD value (computed as the change over 1850–1985 - see methodology for details). Models with an ASR_HD greater than 1.5 W m^{-2} are classified as 'strong' models, and are shown in bold text. Also shown is the *arbitrary* model number assigned in figure 12 of the main paper to aid comparison

Centre	Model	Members	ASR_HD [W m^{-2}]	Model # in Fig.12	Data reference	Model reference
CSIRO	**ACCESS-ESM1-5**	**9**	**1.93**	**9**	**Ziehn et al. (2019)**	**Ziehn et al. (2020)**
BCC	BCC-CSM2-MR	3	0.60	14	Wu et al. (2018)	Wu et al. (2019)
NCAR	**CESM2**	**9**	**2.51**	**5**	**Danabasoglu (2019a)**	**Danabasoglu et al. (2020)**
NCAR	**CESM2-WACCM**	**3**	**2.74**	**7**	**Danabasoglu (2019b)**	**Danabasoglu et al. (2020)**
CNRM-CERFACS	CNRM-CM6-1	9	1.04	13	Voldoire (2018)	Voldoire et al. (2019)
NASA-GISS	**GISS-E2-1-H (p1)**	**9**	**1.67**	**2**	**for Space Studies (NASA/GISS)**	**Kelley et al. (2020), Miller et al. (2021)**
MOHC	**HadGEM3-GC31-LL**	**4**	**2.47**	**1**	**Ridley et al. (2019a)**	**Andrews et al. (2020), Kuhlbrodt et al. (2018)**
MOHC	**HadGEM3-GC31-MM**	**4**	**2.64**	**8**	**Ridley et al. (2019b)**	**Andrews et al. (2020)**
INM	INM-CM5-0	5	0.52	17	Volodin et al. (2019)	Volodin et al. (2017), Volodin and Kostrykin (2016)
IPSL	IPSL-CM6A-LR	9	0.34	12	Boucher et al. (2021)	Boucher et al. (2020)
MIROC	MIROC6	9	0.81	11	Tatebe and Watanabe (2018)	Tatebe et al. (2019)
MPI-M	MPI-ESM1-2-HR	9	0.33	15	Jungclaus et al. (2019)	Mauritsen et al. (2019), Stevens et al. (2013)
MPI-M	MPI-ESM1-2-LR	9	0.01	18	Wieners et al. (2019)	Mauritsen et al. (2019), Stevens et al. (2013)
MRI	**MRI-ESM2-0**	**5**	**2.36**	**6**	**Yukimoto et al. (2019)**	**YUKIMOTO et al. (2019)**
NUIST	NESM3	5	1.28	16	Cao and Wang (2019)	Cao et al. (2018)
NCC	**NorESM2-LM**	**3**	**2.64**	**4**	**Seland et al. (2019)**	**Seland et al. (2020)**
MOHC	**UKESM1-0-LL**	**9**	**2.94**	**3**	**Tang et al. (2019)**	**Sellar et al. (2019)**

2 Additional figures

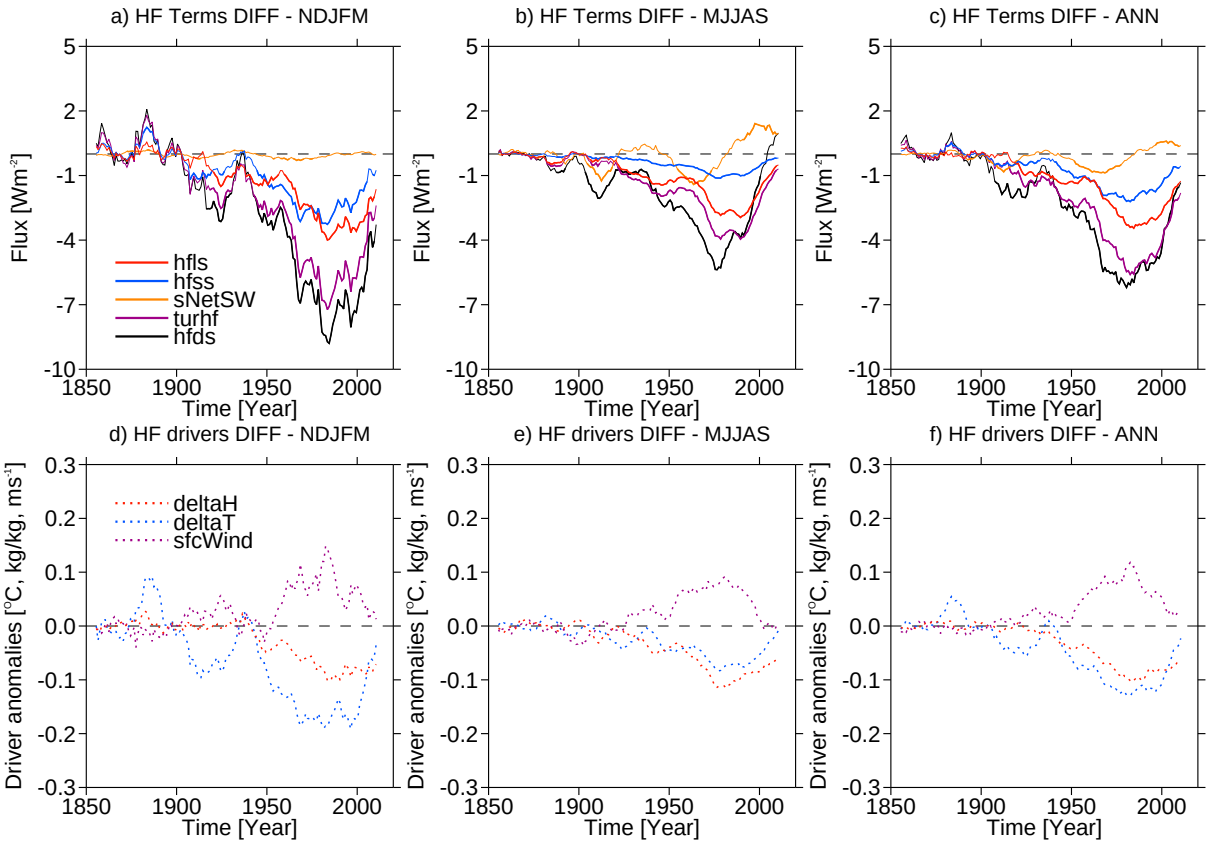

Figure S1: Time evolution of the differences between subpolar surface heat fluxes in 'strong' and 'weak' models and the drivers of turbulent heat fluxes. a) shows winter (Nov–Mar) difference ('strong'–'weak') in anomalous turbulent heat fluxes (turhf, black), surface shortwave (sNetSW, yellow), sensible (hfss, blue) and latent heat (hfls, red) averaged over the SPNA. Anomalies are first made relative to 1850–1879 before taking the difference. b) and c) show the same but now for the summer (May–Sept) and annual mean. d) to f) shows the same as a) to c) but now for the drivers of turbulent heat fluxes. Blue and red dotted lines show the differences in air-sea temperature (ΔT, in °C) and humidity (ΔH, in kg/kg), and purple shows surface wind speed (sfcWind, in m s^{-1}) averaged over the SPNA. Thick lines in a) - c) show where differences are statistically significant at the $p \leq 0.05$ based on a Student's T-test.

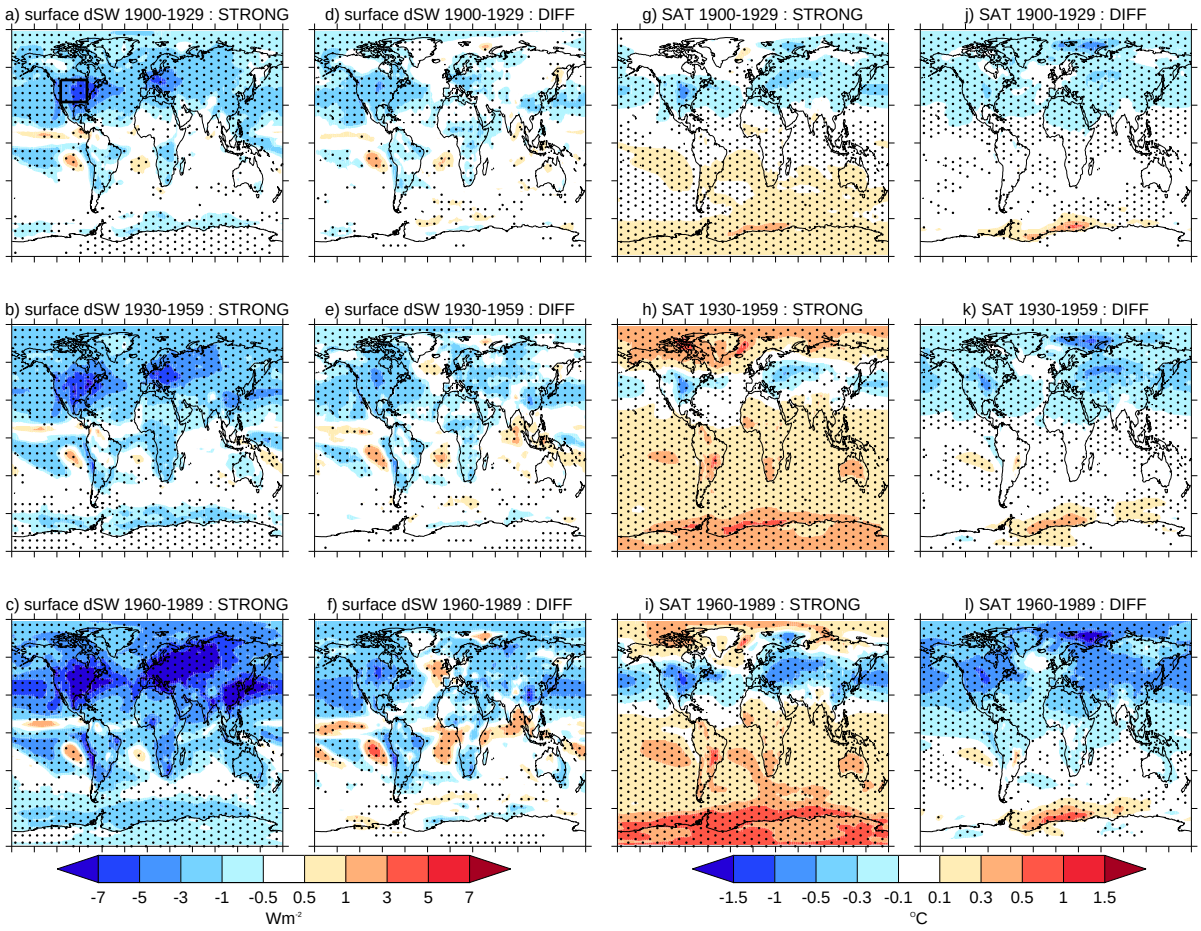

Figure S2: shows the evolution of surface downwelling shortwave anomalies (surface dSW, e.g. CMIP6 variable *rsds*) and surface air temperature (SAT, e.g. CMIP6 variable *tas*) in the 'strong' models and the difference with 'weak' for 30-year time-periods. a) shows the surface dSW anomalies for the 1900–1929 period averaged over 'strong' models. Negative anomalies indicate a reduction in downwelling radiation (i.e. negative radiative forcing). b) and c) shows the same for the 1930–1959 and 1960–1989 periods, respectively. d)–f) shows the same as a)–c) but now for the difference between 'strong' and 'weak' models (i.e., 'strong' *minus* 'weak'). g)–i) shows the same as a)–c) but now for SAT. j)–l) shows the same as d)–f) but now for SAT. Stippling shows where the anomalies are significant at the $p \leq 0.05$ level. All anomalies are relative to 1850–1879.

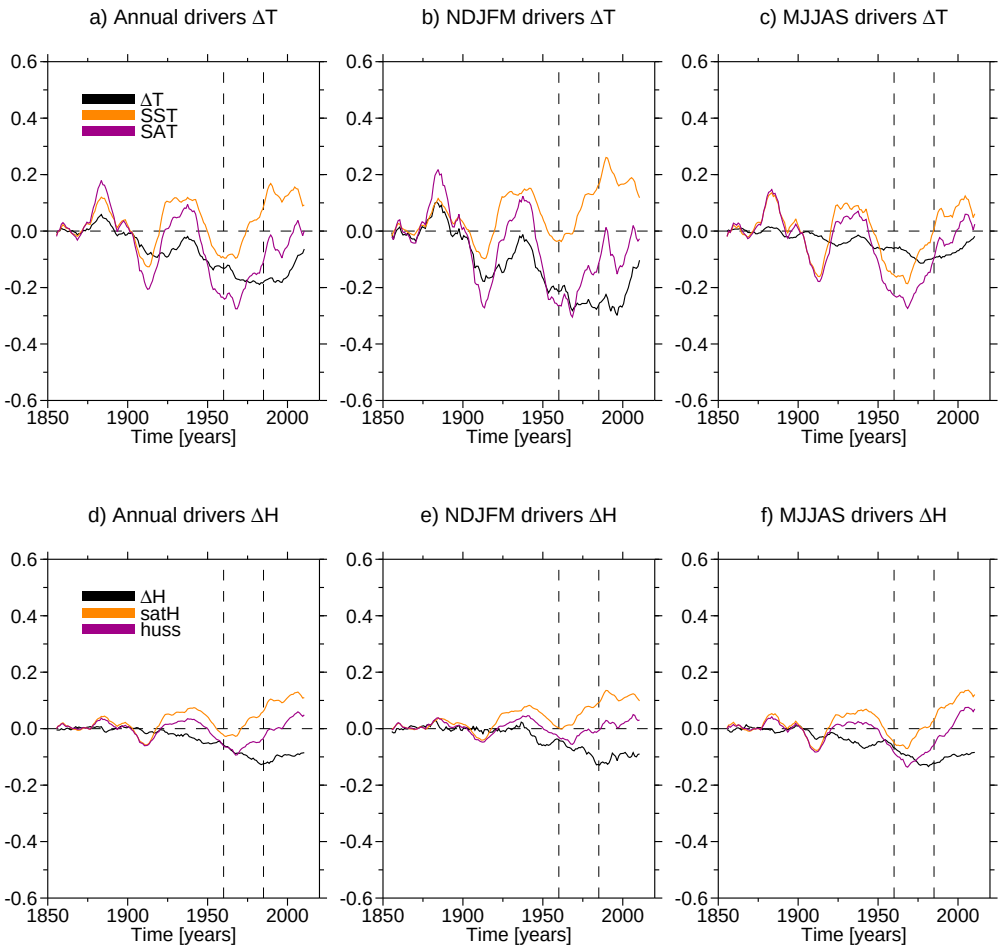

Figure S3: Atmospheric and oceanic drivers of ΔT and ΔH averaged over the SPNA (50-65°N - note the smaller area is chosen to represent the region of positive SST anomalies in figure 5 in the main paper). a) shows the difference in annual-mean ΔT (e.g. SAT *minus* SST, black), SST (orange), and SAT (purple) between the 'strong' and 'weak' ensemble (e.g., 'strong' *minus* 'weak'). b) shows the same but now for ΔH (e.g. huss *minus* satH), surface specific humidity (huss), and saturated humidity (satH) computed from SST. $satH = 0.98\rho^{-1}640380(kg\,m^{-13})e^{-5107.4/SST}$ where ρ is the density of air and assumed to be 1.22 kg m^{-3}(Large and Yeager, 2009). Note that IPSL-CM6 and NESM3 have been removed from panel b) due to problems with humidity data.

References

Andrews, M. B., and Coauthors, 2020: Historical simulations with hadgem3-gc3.1 for cmip6. *Journal of Advances in Modeling Earth Systems*, **12 (6)**, e2019MS001 995, doi:https://doi.org/10.1029/2019MS001995, URL https://agupubs.onlinelibrary.wiley.com/doi/abs/10.1029/2019MS001995, e2019MS001995 10.1029/2019MS001995, https://agupubs.onlinelibrary.wiley.com/doi/pdf/10.1029/2019MS001995.

Boucher, O., and Coauthors, 2020: Presentation and evaluation of the ipsl-cm6a-lr climate model. *Journal of Advances in Modeling Earth Systems*, **12 (7)**, e2019MS002 010, doi:https://doi.org/10.1029/2019MS002010, URL https://agupubs.onlinelibrary.wiley.com/doi/abs/10.1029/2019MS002010, e2019MS002010 10.1029/2019MS002010, https://agupubs.onlinelibrary.wiley.com/doi/pdf/10.1029/2019MS002010.

Boucher, O., and Coauthors, 2021: Ipsl ipsl-cm6a-lr-inca model output prepared for cmip6 cmip historical. Earth System Grid Federation, URL https://doi.org/10.22033/ESGF/CMIP6.13601, doi: 10.22033/ESGF/CMIP6.13601.

Cao, J., and B. Wang, 2019: Nuist nesmv3 model output prepared for cmip6 cmip historical. Earth System Grid Federation, URL https://doi.org/10.22033/ESGF/CMIP6.8769, doi:10.22033/ESGF/CMIP6.8769.

Cao, J., and Coauthors, 2018: The nuist earth system model (nesm) version 3: description and preliminary evaluation. *Geoscientific Model Development*, **11 (7)**, 2975–2993, doi:10.5194/gmd-11-2975-2018, URL https://gmd.copernicus.org/articles/11/2975/2018/.

Danabasoglu, G., 2019a: Ncar cesm2 model output prepared for cmip6 cmip historical. Earth System Grid Federation, URL https://doi.org/10.22033/ESGF/CMIP6.7627, doi:10.22033/ESGF/CMIP6.7627.

Danabasoglu, G., 2019b: Ncar cesm2-waccm model output prepared for cmip6 cmip historical. Earth System Grid Federation, URL https://doi.org/10.22033/ESGF/CMIP6.10071, doi:10.22033/ESGF/CMIP6.10071.

Danabasoglu, G., and Coauthors, 2020: The community earth system model version 2 (cesm2). *Journal of Advances in Modeling Earth Systems*, **12 (2)**, e2019MS001 916, doi:https://doi.org/10.1029/2019MS001916, URL https://agupubs.onlinelibrary.wiley.com/doi/abs/10.1029/2019MS001916, e2019MS001916 2019MS001916, https://agupubs.onlinelibrary.wiley.com/doi/pdf/10.1029/2019MS001916.

for Space Studies (NASA/GISS), N. G. I., 2019: Nasa-giss giss-e2.1h model output prepared for cmip6 cmip historical. Earth System Grid Federation, URL https://doi.org/10.22033/ESGF/CMIP6.7128, doi: 10.22033/ESGF/CMIP6.7128.

Jungclaus, J., and Coauthors, 2019: Mpi-m mpi-esm1.2-hr model output prepared for cmip6 cmip historical. Earth System Grid Federation, URL https://doi.org/10.22033/ESGF/CMIP6.6594, doi: 10.22033/ESGF/CMIP6.6594.

Kelley, M., and Coauthors, 2020: Giss-e2.1: Configurations and climatology. *Journal of Advances in Modeling Earth Systems*, **12 (8)**, e2019MS002 025, doi:https://doi.org/10.1029/2019MS002025, URL https://agupubs.onlinelibrary.wiley.com/doi/abs/10.1029/2019MS002025, e2019MS002025 10.1029/2019MS002025, https://agupubs.onlinelibrary.wiley.com/doi/pdf/10.1029/2019MS002025.

Kuhlbrodt, T., and Coauthors, 2018: The low-resolution version of hadgem3 gc3.1: Development and evaluation for global climate. *Journal of Advances in Modeling Earth Systems*, **10 (11)**, 2865–2888, doi:https://doi.org/10.1029/2018MS001370, URL https://agupubs.onlinelibrary.wiley.com/doi/abs/10.1029/2018MS001370, https://agupubs.onlinelibrary.wiley.com/doi/pdf/10.1029/2018MS001370.

Large, W., and S. Yeager, 2009: The global climatology of an interannually varying air–sea flux data set. *Climate dynamics*, **33 (2-3)**, 341–364, doi:10.1007/s00382-008-0441-3.

Mauritsen, T., and Coauthors, 2019: Developments in the mpi-m earth system model version 1.2 (mpi-esm1.2) and its response to increasing co2. *Journal of Advances in Modeling Earth Systems*, **11 (4)**, 998–1038, doi:https://doi.org/10.1029/2018MS001400, URL https://agupubs.onlinelibrary.wiley.com/doi/abs/10.1029/2018MS001400, https://agupubs.onlinelibrary.wiley.com/doi/pdf/10.1029/2018MS001400.

Miller, R. L., and Coauthors, 2021: Cmip6 historical simulations (1850–2014) with giss-e2.1. *Journal of Advances in Modeling Earth Systems*, **13 (1)**, e2019MS002 034, doi:https://doi.org/10.1029/2019MS002034, URL https://agupubs.onlinelibrary.wiley.com/doi/abs/10.1029/2019MS002034, e2019MS002034 10.1029/2019MS002034, https://agupubs.onlinelibrary.wiley.com/doi/pdf/10.1029/2019MS002034.

Ridley, J., M. Menary, T. Kuhlbrodt, M. Andrews, and T. Andrews, 2019a: Mohc hadgem3-gc31-ll model output prepared for cmip6 cmip historical. Earth System Grid Federation, URL https://doi.org/10.22033/ESGF/CMIP6.6109, doi:10.22033/ESGF/CMIP6.6109.

Ridley, J., M. Menary, T. Kuhlbrodt, M. Andrews, and T. Andrews, 2019b: Mohc hadgem3-gc31-mm model output prepared for cmip6 cmip historical. Earth System Grid Federation, URL https://doi.org/10.22033/ESGF/CMIP6.6112, doi:10.22033/ESGF/CMIP6.6112.

Seland, Ø., and Coauthors, 2020: Overview of the norwegian earth system model (noresm2) and key climate response of cmip6 deck, historical, and scenario simulations. *Geoscientific Model Development*, **13 (12)**, 6165–6200, doi:10.5194/gmd-13-6165-2020, URL https://gmd.copernicus.org/articles/13/6165/2020/.

Seland, y., and Coauthors, 2019: Ncc noresm2-lm model output prepared for cmip6 cmip historical. Earth System Grid Federation, URL https://doi.org/10.22033/ESGF/CMIP6.8036, doi:10.22033/ESGF/CMIP6.8036.

Sellar, A. A., and Coauthors, 2019: Ukesm1: Description and evaluation of the u.k. earth system model. *Journal of Advances in Modeling Earth Systems*, **11 (12)**, 4513–4558, doi:https://doi.org/10.1029/2019MS001739, URL https://agupubs.onlinelibrary.wiley.com/doi/abs/10.1029/2019MS001739, https://agupubs.onlinelibrary.wiley.com/doi/pdf/10.1029/2019MS001739.

Stevens, B., and Coauthors, 2013: Atmospheric component of the mpi-m earth system model: Echam6. *Journal of Advances in Modeling Earth Systems*, **5 (2)**, 146–172, doi:https://doi.org/10.1002/jame.20015, URL https://agupubs.onlinelibrary.wiley.com/doi/abs/10.1002/jame.20015, https://agupubs.onlinelibrary.wiley.com/doi/pdf/10.1002/jame.20015.

Tang, Y., S. Rumbold, R. Ellis, D. Kelley, J. Mulcahy, A. Sellar, J. Walton, and C. Jones, 2019: Mohc ukesm1.0-ll model output prepared for cmip6 cmip historical. Earth System Grid Federation, URL https://doi.org/10.22033/ESGF/CMIP6.6113, doi:10.22033/ESGF/CMIP6.6113.

Tatebe, H., and M. Watanabe, 2018: Miroc miroc6 model output prepared for cmip6 cmip historical. Earth System Grid Federation, URL https://doi.org/10.22033/ESGF/CMIP6.5603, doi:10.22033/ESGF/CMIP6.5603.

Tatebe, H., and Coauthors, 2019: Description and basic evaluation of simulated mean state, internal variability, and climate sensitivity in miroc6. *Geoscientific Model Development*, **12 (7)**, 2727–2765, doi:10.5194/gmd-12-2727-2019, URL https://gmd.copernicus.org/articles/12/2727/2019/.

Voldoire, A., 2018: Cmip6 simulations of the cnrm-cerfacs based on cnrm-cm6-1 model for cmip experiment historical. Earth System Grid Federation, URL https://doi.org/10.22033/ESGF/CMIP6.4066, doi:10.22033/ESGF/CMIP6.4066.

Voldoire, A., and Coauthors, 2019: Evaluation of cmip6 deck experiments with cnrm-cm6-1. *Journal of Advances in Modeling Earth Systems*, **11 (7)**, 2177–2213, doi:https://doi.org/10.1029/2019MS001683, URL https://agupubs.onlinelibrary.wiley.com/doi/abs/10.1029/2019MS001683, https://agupubs.onlinelibrary.wiley.com/doi/pdf/10.1029/2019MS001683.

Volodin, E., and Coauthors, 2019: Inm inm-cm5-0 model output prepared for cmip6 cmip historical. Earth System Grid Federation, URL https://doi.org/10.22033/ESGF/CMIP6.5070, doi:10.22033/ESGF/CMIP6.5070.

Volodin, E. M., and S. V. Kostrykin, 2016: The aerosol module in the inm ras climate model. *Russian Meteorology and Hydrology*, **41 (8)**, 519–528, doi:10.3103/S106837391608001X, URL https://doi.org/10.3103/S106837391608001X.

Volodin, E. M., and Coauthors, 2017: Simulation of the present-day climate with the climate model inmcm5. *Climate Dynamics*, **49 (11)**, 3715–3734, doi:10.1007/s00382-017-3539-7, URL https://doi.org/10.1007/s00382-017-3539-7.

Wieners, K.-H., and Coauthors, 2019: Mpi-m mpi-esm1.2-lr model output prepared for cmip6 cmip historical. Earth System Grid Federation, URL https://doi.org/10.22033/ESGF/CMIP6.6595, doi:10.22033/ESGF/CMIP6.6595.

Wu, T., and Coauthors, 2018: Bcc bcc-csm2mr model output prepared for cmip6 cmip historical. Earth System Grid Federation, URL https://doi.org/10.22033/ESGF/CMIP6.2948, doi:10.22033/ESGF/CMIP6.2948.

Wu, T., and Coauthors, 2019: The beijing climate center climate system model (bcc-csm): the main progress from cmip5 to cmip6. *Geoscientific Model Development*, **12 (4)**, 1573–1600, doi:10.5194/gmd-12-1573-2019, URL https://gmd.copernicus.org/articles/12/1573/2019/.

YUKIMOTO, S., and Coauthors, 2019: The meteorological research institute earth system model version 2.0, mri-esm2.0: Description and basic evaluation of the physical component. *ournal of the Meteorological Society of Japan. Ser. II*.

Yukimoto, S., and Coauthors, 2019: Mri mri-esm2.0 model output prepared for cmip6 cmip historical. Earth System Grid Federation, URL https://doi.org/10.22033/ESGF/CMIP6.6842, doi:10.22033/ESGF/CMIP6.6842.

Ziehn, T., and Coauthors, 2019: Csiro access-esm1.5 model output prepared for cmip6 cmip historical. Earth System Grid Federation, URL https://doi.org/10.22033/ESGF/CMIP6.4272, doi:10.22033/ESGF/CMIP6.4272.

Ziehn, T., and Coauthors, 2020: The australian earth system model: Access-esm1.5. *Journal of Southern Hemisphere Earth Systems Science*, **70 (1)**, 193–214, URL https://doi.org/10.1071/ES19035.